DOI: 10.1002/chem.200901519

Bifunctional Acid–Base Ionic Liquid Organocatalysts with a Controlled Distance Between Acid and Base Sites

Mercedes Boronat, Maria J. Climent, Avelino Corma,* Sara Iborra, Raquel Montón, and Maria J. Sabater[a]

Abstract: Bifunctional acid–base ionic liquid organocatalysts with different distances between the two sites have been synthesised, and their activity for the Knoevenagel condensation has been tested. As has been found to be the case with enzymes, the distance between the acidic and basic sites determines the activity of the bifunctional organocatalyst, and at the optimal distance the reaction rate increases by two orders of magnitude with respect to the purely acidic or basic counterpart organocatalysts. The experimental results have been rationalised through the study of the reaction mechanism of the Knoevenagel condensation between malononitrile and benzaldehyde by means of DFT calculations. It has been found that it consists of two consecutive steps. First, deprotonation of malononitrile on the basic site to obtain a methylene carbanion intermediate takes place, and second, co-adsorption and activation of benzaldehyde on the acid centre of this intermediate followed by the C−C bond-formation reaction. The calculations and the kinetic study indicate that there is an inversion of the rate-controlling step when the distance between the acidic and the basic sites is modified, with a direct implication on the reaction rate.

Keywords: acid–base interactions · density functional calculations · ionic liquids · Knoevenagel condensation · organocatalysis

Introduction

Ionic liquids (ILs) are highly relevant in organic synthesis as environmentally benign solvents.[1] They possess favourable properties such as negligible vapour pressure, high polarity, non-flammability, easy handling and good solvating ability for a wide range of substrates and catalysts. The number of ionic liquids that can be produced is in essence limitless, and the variation in the properties as a consequence of small changes in the molecular structure greatly extend the scope of applications. Besides their interesting physical properties, the fact that some ionic liquids can show acidity or basicity allows them to be also used as solvent and catalysts in several acid- or base-catalysed processes.[2] For instance, over the past decade, chloroaluminate ionic liquids have gained increasing attention as Lewis acid catalysts and they have been used to catalyse a variety of reactions such as alkylation,[3] esterification,[4] acrylation,[5] dimerisations[6] and Diels–Alder.[7] However, the sensitivity of these ILs to water can be a limitation. The first non-chloroaluminate acidic ionic liquid[8] was based on dialkylimidazolium salts with a side chain containing a -SO_3H group, and were used as catalysts and/or solvent in many conventional acid-catalysed reactions such as olefin oligomerisation,[9] etherification,[8] esterification[10] and Friedel–Crafts alkylation.[11] Other types of Brønsted acid ionic liquids refer to those obtained through the combination of a Brønsted acid and a Brønsted base, such as N-protonated 1-alkylimidazolium salts,[12] N-protonated lactams[13] and N-protonated pyridinium salts.[14] These protic ionic liquids have been used in a variety of organic reactions such as esterification,[15] carbonyl protection[16] and Mannich.[17] Recently, an interesting review concerning the properties and applications—including organic reactions—of protic ionic liquids has been reported by Greaves and Drummond.[18] The weak acidity of the C-2 proton in the dialkyl imidazolium ring is also well known and has been anticipated as the cause of some acid catalytic effects.[19]

Basic ionic liquids that form anions of the carboxylate type (such as lactate,[20] formate[21] and acetate), hydroxy anion[22] and dicyanamide[23] have also been prepared. How-

---

[a] Dr. M. Boronat, Dr. M. J. Climent, Prof. A. Corma, Dr. S. Iborra, R. Montón, Dr. M. J. Sabater
Instituto de Tecnología Química (UPV-CSIC)
Av. de los Naranjos s/n, 46022 Valencia (Spain)
Fax: (+34) 96-387-7809
E-mail: acorma@itq.upv.es

ever, there is an alternative in designing ILs with basic sites that incorporate the basic moiety in the cation. These ILs have the advantage of being more thermally stable than those containing basic anions. Thus, a range of salts using a 1-alkyl-4-aza-1-azoniabicyclo[2.2.2]octane cation ($C_n$dabco) in combination with bis(trifluoromethanesulfonyl)amide have been synthesised.[24] Seddon and co-workers have also recently reported a series of basic ILs of formula [Cat^+-Z-Bas][X^-] in which Cat^+ is a positively charged moiety consisting of a heterocyclic ring structure, Bas is a hindered basic moiety that comprises at least one nitrogen, phosphorous, sulphur, oxygen or boron atom, and Z is a carbon chain joining Cat^+ with Bas. The authors claim that these ILs can be used as promoters or catalysts for a variety of reactions such as esterifications, transesterifications, aldol reactions, polymerisations, Robinson annulation, Heck and Suzuki coupling and so on.[25] Finally, proton-conducting non-aqueous electrolytes in fuel cells have been prepared based on bis(trifluoromethanesulfonyl)amide.[26]

gem-Diamines present high pK_a values and have been named as proton sponges.[27] On account of their strong basicity they have been used as organocatalysts for reactions such as Knoevenagel and aldol condensations.[28,29] We have recently shown that by anchoring the *gem*-diamine proton sponge 1,8-bis(dimethylamino)naphthalene (DMAN) on a carrier containing mildly acidic sites, a bifunctional catalyst containing acid and base sites is formed that enhances the rate of the Knoevenagel condensation between benzaldehyde and methylene active compounds.[30] This was shown to occur through a mechanism in which the mildly acidic site of the support activates the benzaldehyde through the carbonyl group, whereas the basic site of the proton sponge was responsible for the activation of the methylene active compound (diethyl malonate) by proton abstraction. In the case of enzymes with acid–base sites, key factors for the enhanced activity are related to the distance between the acid and basic sites and their geometrical configuration. In the case of organic bases supported on acidic carriers, it is difficult to control the above-mentioned factors. However, this should be easier in the case of organocatalysts, in which the distance between the acidic and basic sites can be controlled by the synthesis of the molecule.

In the present work we have synthesised bifunctional acid–base IL organocatalysts with different distances and configuration between the two sites, and which also incorporate the interesting solvent extraction and recyclable properties of ILs. We will show that bifunctional molecules act as active, selective and recyclable catalysts for Knoevenagel condensation reactions. When an optimum distance between the acidic and basic sites exits, the reaction rate increases by two orders of magnitude with respect to the counterpart monofunctional basic catalyst.

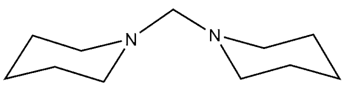
Diamine-A

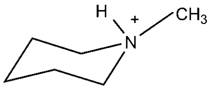
[*N*-Methyl piperidinium]BF_4

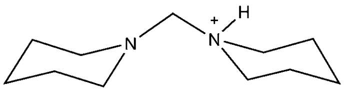
[Diamine-A]BF_4

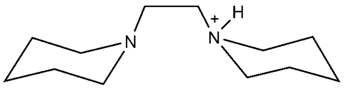
[Diamine-B]BF_4

On the basis of this observation, we thought that it could be of much interest to prepare a bifunctional acid–base organocatalyst with the optimum distance and configuration between the two sites that simultaneously incorporates the interesting solvent extraction and recyclable properties of ILs. In the present work we have synthesised organocatalysts with IL properties that present acidic and basic sites in the same molecule and in which the distance between the acidic and the basic sites has been changed. This bifunctional molecule acts as very active, selective and recyclable catalyst for condensation reactions, thereby increasing the reaction rate by almost two orders of magnitude with respect to the counterpart basic catalyst.

Results and Discussion

Catalytic activity: To check the catalytic activity of the newly synthesised [diamine-A]BF_4 IL in which the acid and basic sites are separated by a -CH_2- group, the Knoevenagel condensation between benzaldehyde and several compounds with active methylene groups and different pK_a values was selected as a test reaction. The Knoevenagel condensation (Scheme 1) is an important carbon–carbon bond-forming reaction that is typically catalysed by base,[31] acid,[32–34] or acid–base catalysts.[35] Then, reactions between benzaldehyde and malononitrile, ethyl cyanoacetate, ethyl acetoacetate and diethyl malonate were performed using [diamine-A]BF_4 IL as catalyst (1 mol%) in the absence of solvent, since the reactants and catalyst form a homogeneous mixture. The results obtained (Figure 1) show that the order of reactivity of the different reactants is in accordance with the decrease in the pK_a value of the methylene active compounds, that is, malononitrile > ethyl cyanoacetate > ethyl acetoacetate > diethyl malonate. The selectivity to the condensation product is 100% in all cases, and the ionic liquid characteristics of [diamine-A]BF_4 allow the extraction and recycling of the catalyst. Indeed, three reaction–extraction cycles using diethyl ether have been performed, and the mass balance was always above 98% without any loss of activity.

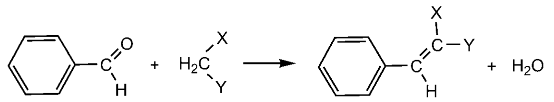

Scheme 1. The Knoevenagel condensation between benzaldehyde and several compounds with active methylene groups (X = CN, CH_3, COOEt; Y = CN, COOEt).

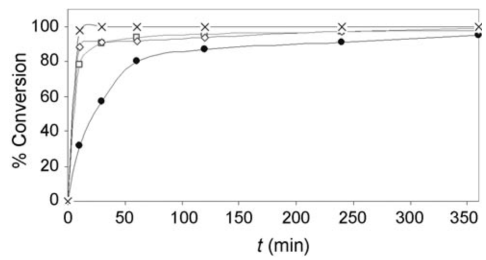

Figure 1. Knoevenagel reactions between benzaldehyde (32 mmol) and different methylene active compounds (28 mmol) in the presence of [diamine-A]BF_4 (0.28 mmol): (×) malononitrile at 25 °C, (◇) ethyl cyanoacetate at 25 °C, (□) methyl acetoacetate at 60 °C, (●) diethyl malonate at 80 °C.

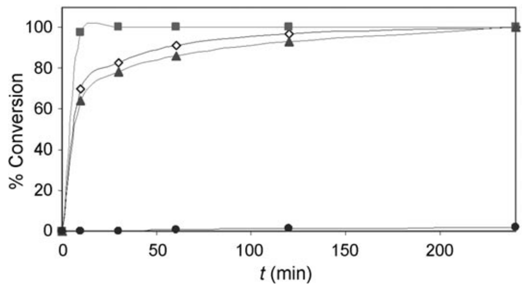

Figure 2. Knoevenagel condensation between benzaldehyde (32 mmol) and malononitrile (28 mmol) in the presence of [N-methyl piperidine]BF_4 (0.28 mmol) (■), diamine-A (◇), [diamine-A]BF_4 (■) and [diamine-B]BF_4 (▲).

For purposes of comparison, the reaction between benzaldehyde and malononitrile was also performed using only [*N*-methyl piperidinium]BF_4 as acid catalyst, or only the highly active *gem*-diamine-A precursor as base catalyst, and the results obtained are presented in Figure 2. According to our previous results, the basic *gem*-diamine-A is more active than the acidic [*N*-methyl piperidinium]BF_4 catalyst, but less active than the acid–base [diamine-A]BF_4 IL. The enhanced activity of the [diamine-A]BF_4 IL can not be attributed to a higher basicity of this molecule, because *gem*-diamine-A is more basic than [diamine-A]BF_4. A key difference between the two organocatalysts is the presence in [diamine-A]BF_4 of a mildly acidic protonated amino group together with the basic site. Indeed, we have seen that the protonated amino groups of [*N*-methyl piperidinium]BF_4 and [diamine-A]BF_4 are acidic enough to catalyse the acetalisation of benzaldehyde with trimethyl orthoformate (TMOF), a reaction typically catalysed by mildly acidic sites, but are not acidic enough to catalyse the Knoevenagel condensation, as demonstrated by the null conversion obtained when performing the Knoevenagel condensation between the different methylene active compounds described above and benzaldehyde in the presence of [*N*-methyl piperidinium]BF_4.

The activity of the protonated compound [diamine-A]BF_4 in the Knoevenagel condensation has been successfully applied to a variety of carbonyl compounds (aldehydes and ketone) as well as different methylene compounds and the results are given in Table 1. In general, the reactions were completed within a few minutes and proceeded very cleanly at room temperature. Indeed the Knoevenagel products were obtained selectively with very high yields.

Table 1. Results obtained in the Knoevenagel condensation of different substrates at room temperature using [diamine-A]BF_4 as catalyst.[a]

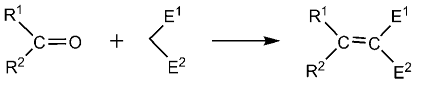

Entry	R^1	R^2	E^1	E^2	*t* [min]	Yield [%][b]
1	Ph	H	$CO_2CH_2CH_3$	$CO_2CH_2CH_3$	20	99
2	*i*-C_3H_7	H	$CO_2CH_2CH_3$	$CO_2CH_2CH_3$	15	99
3	*n*-C_7H_{15}	H	$CO_2CH_2CH_3$	$CO_2CH_2CH_3$	15	100
4	Ph	H	CN	CN	1	100
5	Ph	H	CN	$CO_2CH_2CH_3$	1	100
6	Ph	H	$COCH_3$	$CO_2CH_2CH_3$	10	100
7	CH_3	CH_3	CN	$CO_2CH_2CH_3$	10	100

[a] Reaction conditions: [diamine-A]BF_4 (20 mol %), methylene compound (5 mmol), aldehyde or ketone (5 mmol), room temperature, under nitrogen. [b] Calculated by GC.

In general, the aliphatic aldehydes reacted faster in the Knoevenagel condensation with diethyl malonate than the aromatic benzaldehyde (see entries 1–3 in Table 1), although the yields of the final condensation products were always quantitative. Notably, the reaction rate improved significantly when benzaldehyde was allowed to react with malononitrile, ethyl cyanoacetate and ethyl acetoacetate (see entries 4–6 in Table 1). In all cases studied, the performance of the [diamine-A]BF_4 was clearly superior to that of the 1-butyl-3-methylimidazolium hydroxide ([BmIm]OH) catalyst reported in the literature since the condensation products were obtained with very high yields and shorter times than with [BmIm]OH.[22a]

Since the excellent catalytic results for the Knoevenagel condensation obtained with the bifunctional [diamine-A]BF_4 are difficult to explain through the independent action of the acidic and basic sites present in the organocatalyst, a combined acid–base-catalysed mechanism could be proposed in which the weak Brønsted acid site associated with the N-protonated amino group interacts with the benzaldehyde carbonyl group, thereby polarising the C=O bond and increasing the net positive charge on the C atom. This polarisation makes this C atom more likely to be attacked by the methylene carbanion intermediate formed on the vicinal Lewis basic site associated with the neighbour amine group (Scheme 2).

If the bi-site mechanism is operative, one can expect that the distance between the acidic and basic sites should be a critical parameter in achieving the stabilisation of the transition state involved in the mechanism, just as it occurs in many enzymatic processes. We have studied this effect by synthesising an analogous diamine IL, [diamine-B]BF_4, in which the two nitrogen atoms are separated by a -CH_2–

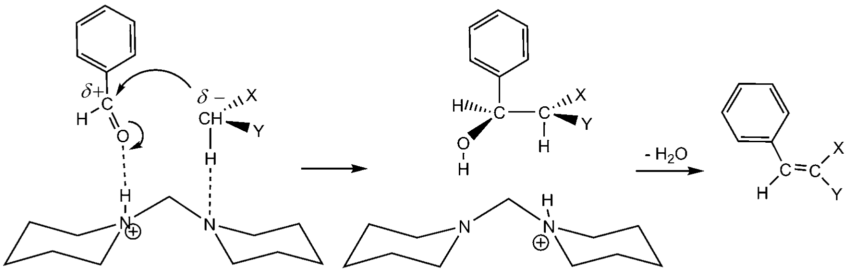

Scheme 2. The bifunctional acid–base mechanism proposed for the Knoevenagel condensation shown in Scheme 1.

CH_2- chain instead of one -CH_2- bridge. Table 2 offers an overview of the physical properties of these organic salts.

Table 2. Properties of organic salts [diamine-A]BF_4, [diamine-B]BF_4 and [*N*-methyl piperidinium]BF_4.

Organic salt	*T* (dec) [°C][a]	ρ [$g\,cm^{-3}$][b]	Physical state[c]	M.p. [°C]	σ [$\mu S\,cm^{-1}$][d]
[diamine-A]BF_4	120, 307, 392, 437	1.195	solid	108.8	167.0
[diamine-B]BF_4	303, 344, 387	1.196	solid	72	88.4
[*N*-methyl piperidinium]BF_4	–[e]	1.215	liquid	–	137.0

[a] Decomposition temperatures were obtained from thermogravimetric analysis under an N_2 flow (rate: 10°C min^{-1}). [b] Calculated at 30°C. [c] Physical state at 20°C. [d] Ionic conductivity calculated on 10^{-3} M aqueous solutions at 20°C. [e] Not determined.

The acidity of the [diamine-B]BF_4 salt was first tested by performing the acetalisation reaction of benzaldehyde with TMOF. The activity obtained with [diamine-B]BF_4 was similar to that measured for [diamine-A]BF_4, thus indicating a similar acidity for both catalysts. However, when the Knoevenagel condensation between malononitrile and benzaldehyde was performed at 25°C with [diamine-B]BF_4, the yield was much lower than that with the [diamine-A]BF_4 catalyst (see Figure 2). Moreover, when diethyl malonate was used as the reagent, only 1% yield of the Knoevenagel adduct was observed after a 6 h reaction time with [diamine-B]BF_4, whereas 85% yield was obtained with [diamine-A]BF_4, which results in a catalytic activity more than two orders of magnitude larger.

Several conclusions can be extracted from these results. First, it appears that the BF_4^- anion, which in principle could act as a weak base, does not play any key role as basic catalytic site in the reaction. Secondly, the results corroborate that a purely acidic mechanism is not acting in the process. Finally, and most importantly, it appears that there is an optimal distance between the acidic and basic sites to achieve their cooperative effect. In an attempt to check this hypothesis and find the optimal distance between both active centres, the reaction mechanism was studied by means of density functional calculations.

Computational study of the reaction mechanism: The mechanism of the Knoevenagel condensation between benzaldehyde and malononitrile catalysed by [diamine-A]BF_4 and [diamine-B]BF_4 was investigated theoretically by means of DFT calculations. According to the bifunctional acid–base mechanism proposed above and depicted in Scheme 2, it was initially assumed that the carbonyl group of benzaldehyde would interact with the N-protonated acidic site, and malononitrile would adsorb on the basic neighbouring N atom. The optimised geometry of the complex formed by co-adsorption of benzaldehyde and malononitrile on [diamine-A]BF_4 is depicted in Figure 3. The carbonyl group of benzaldehyde interacts with the proton of the N-protonated site, and as a result the carbonyl group is polarised and the C=O bond length increases from 1.214 Å in the gas phase to 1.228 Å. The calculated $O_{(CO)}$–$H_{(NH)}$ distance is short (1.856 Å), whereas the distance between the H atom of malononitrile and the basic N atom of the diamine is considerably larger (2.286 Å). The different strength of the two interactions involved, namely, the benzaldehyde acidic site and malononitrile basic site, is also reflected in the calculated adsorption energies: −8.8 kcal mol^{-1} for benzaldehyde on the acidic site and only −2.6 kcal mol^{-1} for co-adsorption of malononitrile on the basic N of the benzaldehyde–[diamine-A]BF_4 complex. Benzaldehyde adsorption on the acidic proton of [diamine-B]BF_4 is exothermic by 5.3 kcal mol^{-1}, but interaction of malononitrile with the basic site of the benzaldehyde–[diamine-B]BF_4 complex is negligible, and no minimum corresponding to such a system could be obtained. Moreover, despite all our efforts, it was not possible to find a reaction path that, starting from the benzaldehyde–malononitrile–[diamine-A]BF_4 complex (Figure 3) and through a simultaneous deprotonation of malononitrile and attack of the negatively charged carbon atom to the carbon atom of the carbonyl group, yields the condensation alcohol intermediate shown in Scheme 2. Instead, it was found that the mechanism consists of two steps: 1) deprotonation of adsorbed malononitrile to yield a methylene carbanion intermediate that remains adsorbed on a positively charged diprotonated diamine, and 2) co-adsorption of benzaldehyde on this system and reaction with the

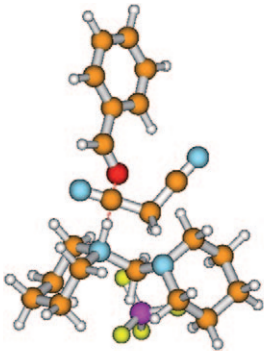

Figure 3. Optimised geometry of benzaldehyde and malononitrile co-adsorbed on [diamine-A]BF_4: O red, C orange, N blue, H white, B pink, F yellow.

methylene carbanion to form a condensation alcohol intermediate.

The species involved in the first step of the mechanism and the calculated energy profiles are depicted in Figures 4 and 5, respectively, and the adsorption, activation and reaction energies are summarised in Table 3. Initially, malononitrile interacts with the acid proton of [diamine-A]BF_4 through the lone pair of electrons on the N atom of one of the C≡N groups, thereby forming an adsorption complex (M-DA) 3.6 kcal mol^{-1} more stable than the separated reactants. Then, the basic N of [diamine-A]BF_4 abstracts one of the hydrogen atoms of malononitrile through the transition state depicted in Figure 4b (TS1-DA) and a methylene carbanion intermediate (I1-DA) is formed (Figure 4c). In the transition state, the $C_{(methylene)}$–H and H–$N_{(diamine)}$ distances involving the hydrogen atom that is being transferred are 1.463 and 1.275 Å, respectively, and the proton of the N-protonated amino group continues to interact with one of the C≡N groups of malononitrile. In the methylene carbanion intermediate I1-DA, the N atom of this C≡N group is hydrogen bonded to the two protons of the diprotonated [diamine-A]BF_4, with calculated $N_{(CN)}$–$H_{(diamine)}$ distances of 1.591 and 1.601 Å, and with a concomitant increase in the CN bond length from 1.159 Å in the gas phase to 1.196 Å. Moreover, an important electronic reorganisation occurs spontaneously as the geometry of the system is optimised. The negative charge that should be localised on the tri-coordinated carbon atom, which is not involved in any interaction, moves to the N atom that is interacting with the diamine protons, the triple C≡N bond is converted into a double bond, and a new C=C double bond is formed. The calculated activation energy for this step is 10.9 kcal mol^{-1}, and the reaction intermediate is only 0.7 kcal mol^{-1} more stable than the transition state. The low stability of the reaction intermediate can be explained by the strong repulsive interaction that exists between the two positive charges in the diprotonated diamine, which are localised on the N-protonated atoms and are separated by only 2.469 Å.

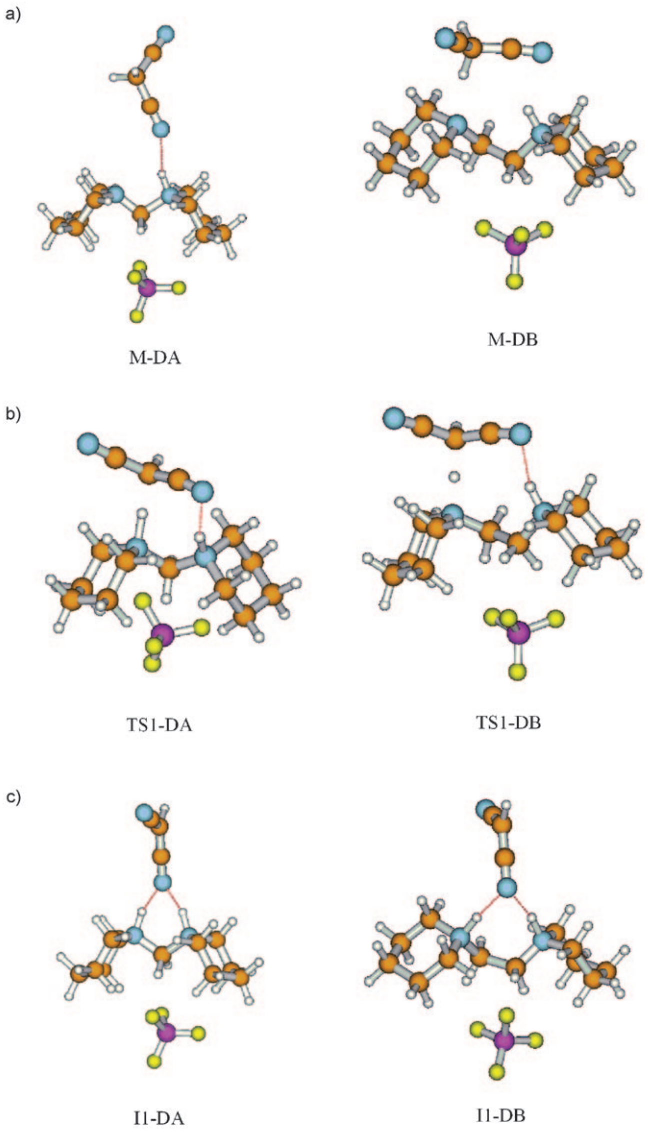

M-DA M-DB

TS1-DA TS1-DB

I1-DA I1-DB

Figure 4. a) Adsorbed malononitrile, b) transition state for deprotonation and c) adsorbed methylene carbanion intermediate on [diamine-A]BF_4 (left) and [diamine-B]BF_4 (right: C orange, N blue, H white, B pink, F yellow.

The process is not completely equivalent when [diamine-B]BF_4 is used as catalyst. In the initial adsorption complex (M-DB), the acidic proton of [diamine-B]BF_4 interacts with one of the C≡N groups, whereas one of the hydrogen atoms of malononitrile adsorbs on the basic N centre of the diamine. Both interactions are weak, so that the calculated adsorption energy is only 0.5 kcal mol^{-1}. However, the molecular conformation is very favourable for the hydrogen-transfer process, and therefore the calculated activation energy is low (1.9 kcal mol^{-1}). As in the methylene carbanion intermediate I1-DA, the negative charge in the reaction intermediate I1-DB is not localised on the tri-coordinated C atom, but on the N atom that interacts with the two protons of the diprotonated [diamine-B]BF_4. The optimised geometry of the methylene carbanion fragment in I1-DA and I1-DB is similar, and the $N_{(CN)}$–$H_{(diamine)}$ distances are slightly longer in the case of [diamine-B]BF_4 (1.629 and 1.663 Å). The main difference between the two intermediate complexes is found in the $N_{(diamine)}$–$N_{(diamine)}$ distance (2.469 in I1-DA and 3.300 Å in I1-DB). This is the distance between the two N atoms bearing the positive charge in the diprotonated diamines, and explains the higher stability of the reaction intermediate with a larger charge separation, namely, I1-DB. Thus, whereas step 1 is clearly endothermic when catalysed by [diamine-A]BF_4 (see Figure 5 and Table 3), it is energetically favourable with [diamine-B]BF_4.

The second step in the reaction mechanism involves adsorption of benzaldehyde on the adsorbed methylene carbanion intermediate complex formed in the first elementary step, and attack of the methylene carbanion onto the carbonyl group to form a condensation alcohol intermediate. The co-adsorbed reactants (R-DA and R-DB), the transition

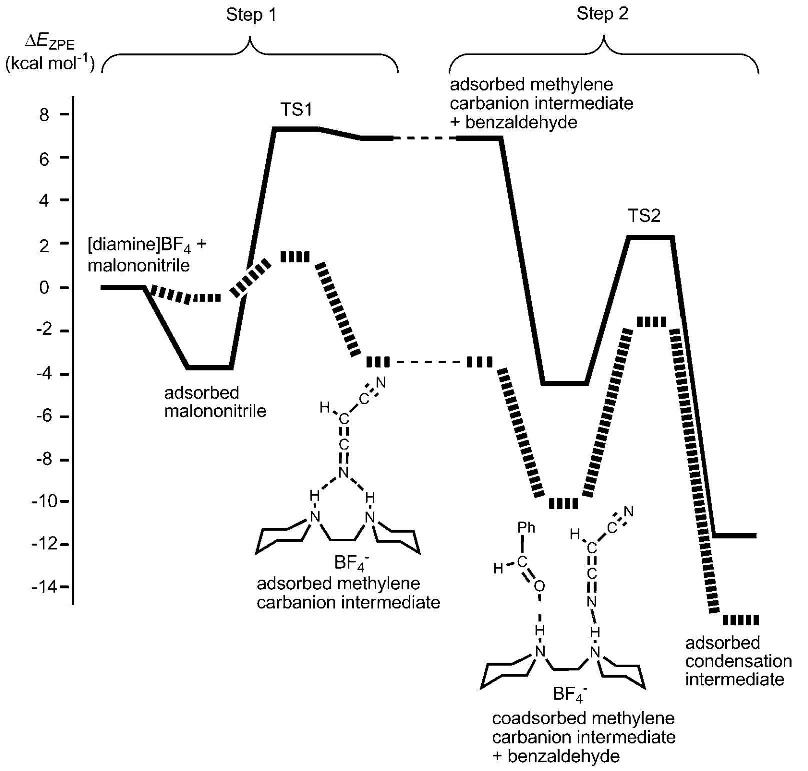

Figure 5. Calculated energy profile for the condensation of malononitrile and benzaldehyde catalysed by [diamine-A]BF_4 (full line) and [diamine-B]BF_4 (dashed line).

Table 3. Calculated adsorption, reaction and activation energies (in kcal mol^{-1}) for the two steps of the mechanism catalysed by [diamine-A]BF_4 and [diamine-B]BF_4.

	[Diamine-A]BF_4		[Diamine-B]BF_4	
	Step 1	Step 2	Step 1	Step 2
adsorption energy	−3.62	−10.83	−0.50	−6.64
activation energy	10.92	6.68	1.92	8.64
reaction energy	10.23	−7.18	−2.90	−5.51

states for the process (TS2-DA and TS2-DB) and the condensation intermediates (I2-DA and I2-DB) are depicted in Figure 6, and the calculated adsorption, activation and reaction energies are summarised in Table 3. In the case of [diamine-A]BF_4, benzaldehyde shows a strong tendency to adsorb on one of the acidic protons of the intermediate complex I1-DA obtained in the first step, thereby partially displacing the methylene carbanion. Irrespectively of the initial distance and orientation of benzaldehyde with respect to the intermediate complex, geometry optimisation always leads to a very stable structure (R-DA, Figure 6a) in which the carbonyl group is hydrogen bonded to one of the protons of the diamine, and deprotonated malononitrile is interacting with the other acidic proton through one of the C≡N groups. The $C_{(CO)}$–$C_{(methylene)}$ distance is 4.518 Å and the relative orientation of both molecules is very favourable for the condensation reaction. The molecular geometry of the transition state (TS2-DA) is quite similar, with the carbonyl group highly activated ($r_{CO}=1.270$ Å), the proton beginning to be transferred ($N_{(diamine)}$–$H_{(diamine)}=1.115$ Å, $H_{(diamine)}$–$O_{(CO)}=1.447$ Å) and the carbonyl and methylene carbon atoms being separated by only 2.235 Å. The product obtained in this process (I2-DA) is an alcohol adsorbed on the initial [diamine-A]BF_4 catalyst and stabilised by two acid–base interactions: one between the N-protonated acidic centre of the diamine and one of the C≡N groups, which also exist in R-DA and TS2-DA, and another one between the H atom of the hydroxyl group and the basic nitrogen of the catalyst. The activation energy obtained for this step is 6.7 kcal mol^{-1}, and the alcohol intermediate formed is 7.2 kcal mol^{-1} more stable than adsorbed reactants.

Adsorption of benzaldehyde on the I1-DB intermediate is weaker than on I1-DA, and different in nature. Benzaldehyde is not able to displace the methylene carbanion from the acidic protons of the diprotonated [diamine-B]BF_4, and the carbonyl group can only interact with the hydrogen atoms of the cyclohexane ring, with a calculated adsorption energy of 6.6 kcal mol^{-1}. However, the optimised geometry of the transition state TS2-DB is similar to that of TS2-DA. The carbonyl group is strongly interacting with the acidic centre ($r_{CO}=1.270$ Å, $H_{(diamine)}$–$O_{(CO)}=1.536$ Å) and the methylene and carbonyl carbon atoms are separated only by 2.174 Å. The activation barrier is 8.6 kcal mol^{-1}, and the intermediate formed is 5.5 kcal mol^{-1} more stable than the separated reactants. In this case, the reaction intermediate is not an adsorbed alcohol, but an alcoholate, since the proton transfer from the diamine has not occurred yet.

The complete energy profile for the condensation of benzaldehyde and malononitrile catalysed by [diamine-A]BF_4 and [diamine-B]BF_4 is depicted in Figure 5. Malononitrile adsorption on [diamine-A]BF_4 is exothermic, but the activation energy necessary for its deprotonation is high, and the methylene carbanion intermediate is a very unstable species. Adsorption of benzaldehyde on this system is energetically very favourable, and the activation energy for the C–C bond formation is lower than the backward desorption of benzaldehyde. This, together with the favourable orientation of the reactants in the R-DA complex, suggests that the second step of the mechanism will be fast, and step 1 will be

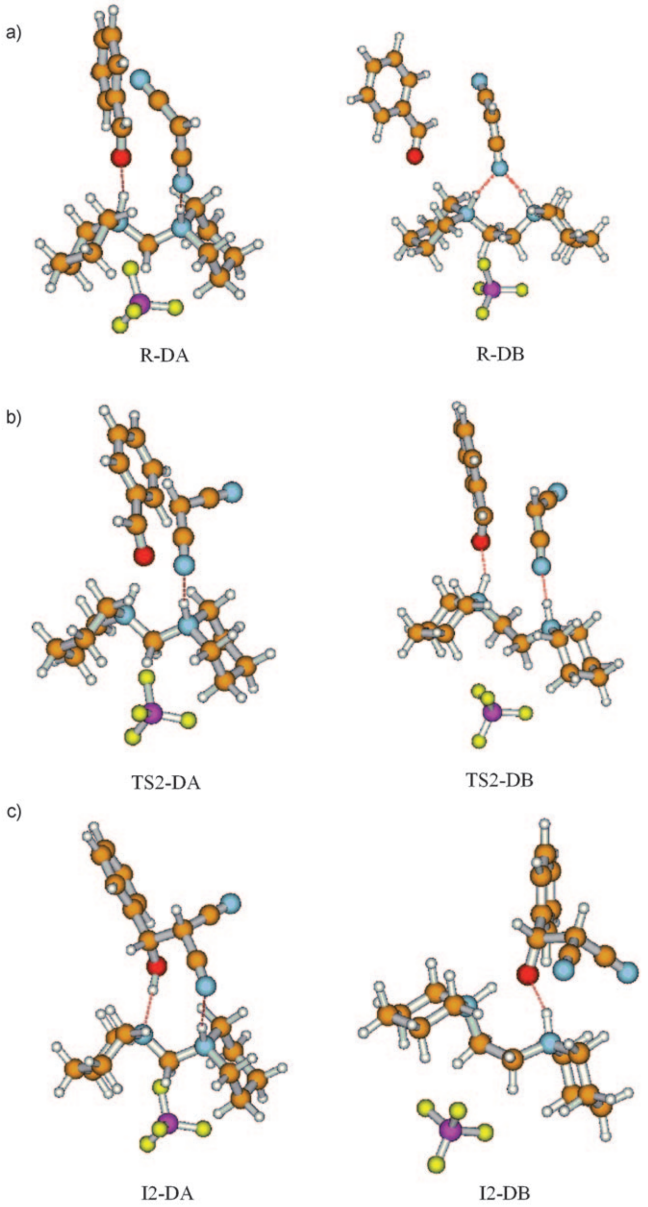

Figure 6. a) Co-adsorbed benzaldehyde and methylene carbanion intermediate, b) transition state for the C–C bond formation and c) condensation alcohol intermediate on [diamine-A]BF_4 (left) and [diamine-B]BF_4 (right): O red, C orange, N blue, H white, B pink, F yellow.

the rate-determining step. On the other hand, malononitrile adsorption on [diamine-B]BF_4 is not very favourable, but the deprotonation step involves a low energy barrier and the reaction intermediate obtained is more stable than the initial reactants, thus suggesting that step 1 is fast with this catalyst. Subsequent adsorption of benzaldehyde on the adsorbed methylene carbanion intermediate is exothermic, but not enough so as to overcome the activation barrier involved in the C–C bond-forming process. More energy is needed for the reaction to proceed, and therefore step 2 is the rate-determining step on this catalyst. Moreover, as previously discussed, benzaldehyde does not directly interact with the acidic site in the R-DB complex, thereby suggesting that entropy effects could have a strong influence on the observed reaction rate. To confirm the proposed mechanism and to check the influence of entropy effects on the catalytic behaviour of the two diamines, a kinetic study of the reaction including the experimental determination of the activation energies was carried out.

Kinetic study: The kinetics of the Knoevenagel condensation between benzaldehyde and malononitrile catalysed by [diamine-A]BF_4 and [diamine-A]BF_4 were studied at different temperatures to obtain experimental activation energies. According to the mechanism proposed by the theoretical study, the first step is adsorption of malononitrile (M) on the diamine catalyst (cat.) [Eq. (1)] and deprotonation of the adsorbed malononitrile ([M–cat.]) to obtain the methylene carbanion intermediate ([I1–cat.]) with a rate constant k_1 [Eq. (2)]; and the second step is co-adsorption of benzaldehyde (B) on the [I1–cat.] intermediate to form a reactant complex ([R–cat.]) [Eq. (3)] that is converted into the condensation intermediate ([I2–cat.]) with a rate constant k_2 [Eq. (4)]:

$$\mathrm{M} + \mathrm{cat.} \xleftrightarrow{K_1} [\mathrm{M}-\mathrm{cat.}] \tag{1}$$

$$[\mathrm{M}-\mathrm{cat.}] \xrightarrow{k_1} [\mathrm{I1}-\mathrm{cat.}] \tag{2}$$

$$[\mathrm{I1}-\mathrm{cat.}] + \mathrm{B} \xleftrightarrow{K_2} [\mathrm{R}-\mathrm{cat.}] \tag{3}$$

$$[\mathrm{R}-\mathrm{cat.}] \xrightarrow{k_2} [\mathrm{I2}-\mathrm{cat}]. \tag{4}$$

Owing to the extremely large reaction rates obtained even at the lowest temperature and catalyst concentration allowed by the experimental setup, a number of approximations were used to simplify the kinetic rate equations and to obtain useful information. When the catalyst used is [diamine-A]BF_4, the rate-determining step is malononitrile deprotonation [Eq. (2)], which is directly dependent upon the concentration of adsorbed malononitrile. Assuming that the adsorption equilibrium [Eq. (1)] is fast and complete, and since the catalyst concentration is constant, the reaction rate (r) could be simplified to give Equation (5):

$$r = \frac{-\mathrm{d}[\mathrm{M}]}{\mathrm{d}t} = k_1[\mathrm{M}] \tag{5}$$

and the experimental results should be fitted to Equation (6)]:

$$\ln[\mathrm{M}] = \ln[\mathrm{M}]_0 - k_1 t \tag{6}$$

On the other hand, with [diamine-B]BF_4 catalyst, malononitrile deprotonation is fast and therefore it can be assumed that the concentration of the intermediate [I1–cat.] is constant and equal to the initial concentration of the catalyst. The rate-determining step [Eq. (4)] depends on the concentration of the reactant complex [R–cat.], which, according to Equation (3), is directly proportional to the concentration of benzaldehyde. Thus, the reaction rate on [diamine-B]BF$_4$ could be simplified to give Equation (7):

$$r = \frac{-\mathrm{d}[\mathrm{M}]}{\mathrm{d}t} = \frac{-\mathrm{d}[\mathrm{B}]}{\mathrm{d}t} = k_2[\mathrm{B}] \tag{7}$$

and the experimental data should fit a first-order equation [Eq. (8)]:

$$\ln[\mathrm{B}] = \ln[\mathrm{B}]_0 - k_2 t \tag{8}$$

Finally, we have also considered the one-step mechanism initially proposed (Scheme 2), in which malononitrile and benzaldehyde co-adsorb on the diamine with the simultaneous occurrence of malononitrile deprotonation and attack onto benzaldehyde to give the condensation intermediate. In this case, the reaction rate would depend on the concentration of both reactants [Eq. (9)]:

$$r = \frac{-\mathrm{d}[\mathrm{M}]}{\mathrm{d}t} = \frac{-\mathrm{d}[\mathrm{B}]}{\mathrm{d}t} = k_3[\mathrm{M}][\mathrm{B}] \tag{9}$$

and using initial concentrations $[\mathrm{M}]_0 = [\mathrm{B}]_0$, the experimental data should fit a second-order equation [Eq. (10)]:

$$\frac{1}{[\mathrm{M}]} - \frac{1}{[\mathrm{M}]_0} = \frac{1}{[\mathrm{B}]} - \frac{1}{[\mathrm{B}]_0} = k_3 t \tag{10}$$

The plots of ln[M] and 1/[M] versus time depicted in Figure 7 for both diamines indicate that when [diamine-A]BF$_4$ is used as catalyst, the reaction rate is first-order with respect to the concentration of malononitrile, thus supporting the two-step mechanism that arises from the theoretical study. The situation is not so clear when the reaction is catalysed by [diamine-B]BF$_4$. In this case, the fitting of the experimental data to the two models is of a similar quality, with $r^2 = 0.989$ for the first-order reaction, and $r^2 = 0.977$ for the second-order reaction. This suggests that competitive adsorption on the active centres or entropy effects related with co-adsorption of the reactants could be quite relevant when the reaction is catalysed by [diamine-B]BF$_4$, as will be seen later.

Activation energies (E_{act}) were calculated from the measured rate constants at different temperatures (T) according to Equations (11) and (12) (in which A is the frequency factor and R is the gas constant):

$$k = A\mathrm{e}^{-E_{\mathrm{act}}/RT} \tag{11}$$

$$\ln k = \ln A - \frac{E_{\mathrm{act}}}{R}\left(\frac{1}{T}\right) \tag{12}$$

as depicted in Figure 8. The quality of the fitting is good in all cases, and the activation energies obtained from the slope of the plot are 8.4 kcal mol^{-1} for [diamine-A]BF$_4$, 7.1 kcal mol^{-1} for [diamine-B]BF$_4$ using the first-order rate constants and 10.2 kcal mol^{-1} for [diamine-B]BF$_4$ using the second-order rate constants. At this point, it is still not possible to definitively state which is the reaction mechanism followed with [diamine-B]BF$_4$. However, there is an important difference when considering the first- and second-order mechanisms with [diamine-B]BF$_4$. In the case of a second-order mechanism, a isokinetic point must exist at a reaction temperature of 38 °C in which the reaction rates on [diamine-A]BF$_4$ and [diamine-B]BF$_4$ are the same (see Figure 8) and at temperatures higher than 38 °C the reaction should be faster on [diamine-B]BF$_4$. On the other hand, when the first-order mechanism is considered, the isokinetic point between the two catalysts should occur at a lower (−11 °C) reaction temperature. To check this hypothesis, the initial reaction rates with both diamines were measured at different temperatures between −10 and 60 °C. The results from Table 4 clearly indicate that the reaction is faster on [diamine-A]BF$_4$ over the whole temperature range, and that at −10 °C the reaction rates for the two catalysts are very close, thus confirming the existence of an isokinetic point at the temperature predicted by the first-order

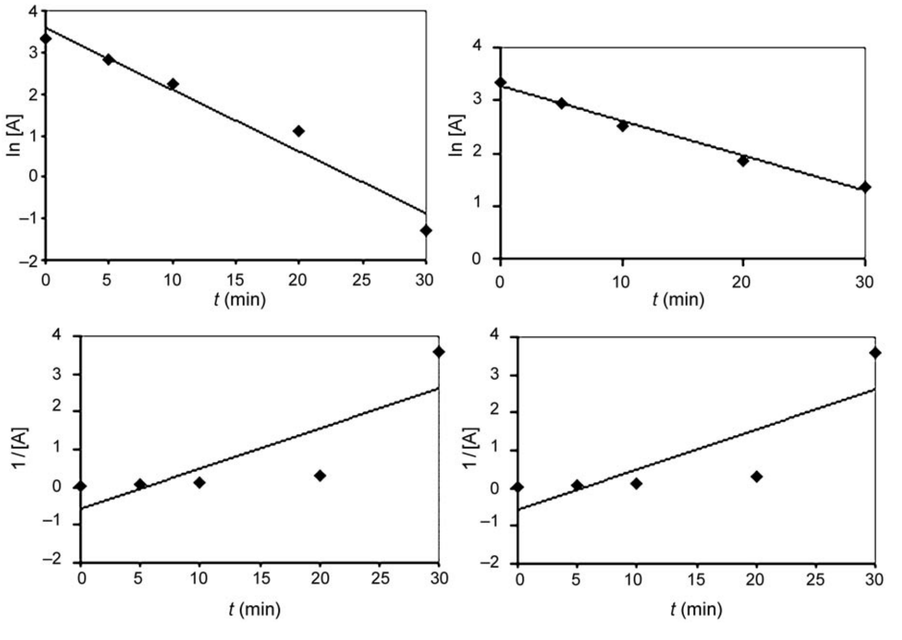

Figure 7. Plots of ln[A] and 1/[A] versus time for the Knoevenagel condensation of malononitrile and benzaldehyde catalyzed by [diamine-A]BF$_4$ (left) and [diamine-B]BF$_4$ (right) at 25 °C. [A] (in mmol L^{-1}) is the malononitrile concentration for [diamine-A]BF$_4$ and the benzaldehyde concentration for [diamine-B]BF$_4$.

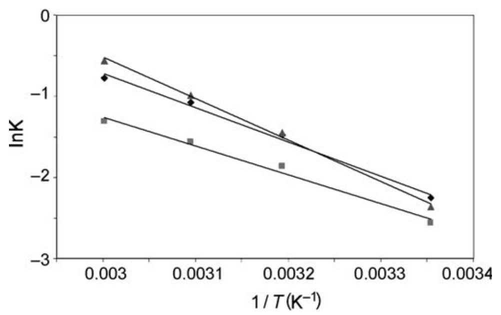

Figure 8. Relationship between rate constants and temperature for the Knoevenagel condensation of malononitrile and benzaldehyde catalysed by [diamine-A]BF_4 (◆) and [diamine-B]BF_4 assuming first-order (■) or second-order (▲) reaction rates.

Table 4. Conversion [%] at different temperatures.

T [°C]	[Diamine-A]BF_4	[Diamine-B]BF_4
−10	7	9
0	28	16
25	41	32
40	68	54
50	82	65
60	90	74

model. It can then be concluded that on both catalysts the reaction follows the two-step mechanism proposed by the theoretical study, and that the different catalytic behaviour arises from a change in the rate-determining step when the distance between the acidic and basic sites is modified.

Comparison of the experimental activation energies with those calculated above is not straightforward, since the mechanism consists of several elementary steps including adsorption processes and consecutive reactions with different activation barriers. But it can be seen in Table 5 that the experimental activation energies correlate well with those calculated for the rate-determining step on each catalyst (step 1 on [diamine-A]BF_4 and step 2 on [diamine-B]BF_4) and are approximately 2 $kcal\,mol^{-1}$ higher for [diamine-A]BF_4 than for [diamine-B]BF_4. The experimental observation that the reaction proceeds faster on the catalyst that involves a higher activation energy is explained by a larger frequency factor [A in Equation (11)] with this catalyst that must be related to entropy (S) effects according to Equation (13) in which k_B is the Boltzmann constant and h is the Planck constant:

Table 5. Calculated and experimental activation energies (in $kcal\,mol^{-1}$) for the two steps involved in the mechanism of the Knoevenagel condensation of malononitrile and benzaldehyde catalysed by [diamine-A]BF_4 and [diamine-A]BF_4.

	[Diamine-A]BF_4		[Diamine-B]BF_4	
	Step 1	Step 2	Step 1	Step 2
calculated	10.92	6.68	1.92	8.64
experimental	8.4	fast	fast	7.1

$$A = \frac{k_\mathrm{B}T}{h} e^{\Delta S^{\neq}}/R \qquad (13)$$

Indeed, the frequency factor A obtained for [diamine-A]BF_4 from the plot in Figure 8 is an order of magnitude larger than that obtained for [diamine-B]BF_4, and this difference must be related to the entropy effects associated with the adsorption and reaction of benzaldehyde on the methylene carbanion intermediates I1-DA and I1-DB. As previously discussed, benzaldehyde adsorbs strongly on the acidic site of intermediate I1-DA, thereby adopting a very favourable orientation for the condensation reaction, so that the entropy effects in the second step of the mechanism are negligible and the reaction rate on [diamine-A]BF_4 only depends on the rate of step 1, which is determined by the activation energy. Adsorption of benzaldehyde on I1-DB is weaker and the relative orientation of the two molecules in the reactant complex R-DB is not so favourable (see Figure 6). When passing from the reactant complex R-DB to the transition state TS2-DB, benzaldehyde has to get very close to the diamine acidic site and to the methylene fragment, with a consequent entropy loss that is reflected in a smaller frequency factor and therefore a lower reaction rate.

Conclusion

Two different bifunctional organocatalysts with ionic liquid properties that contain an acidic and a basic site in the same molecule but with different distances between the two sites have been synthesised, and their activity for the Knoevenagel condensation between benzaldehyde and methylene active compounds has been investigated and compared with that of the purely acidic or basic counterpart organocatalysts. It has been found that the best bifunctional acid–base catalyst is more active than the corresponding monofunctional acid or base catalyst. As has been found to be the case with enzymes, the distance between the acidic and basic sites is a determinant of the activity of the bifunctional organocatalyst. The optimum distance between the two sites and molecular configuration have been rationalised through the study of the molecular mechanism of the Knoevenagel condensation between malononitrile and benzaldehyde by means of DFT calculations. It has been found that it consists of two consecutive steps: 1) deprotonation of malononitrile on the basic site to obtain a methylene carbanion intermediate, and 2) co-adsorption and activation of benzaldehyde on the acidic centre of this intermediate followed by the C−C bond-formation reaction. The calculations indicate that there is an inversion of the rate-controlling step when the distance between the acidic and the basic sites is modified, with a direct effect on the reaction rate. Thus, with [diamine-A]BF_4, in which the acidic and basic sites are separated by a -CH_2- group, malononitrile deprotonation is the most difficult step of the mechanism and requires an activation energy of approximately 11 $kcal\,mol^{-1}$. But once deprotonation occurs, benzaldehyde co-adsorption on the highly unstable methylene carbanion intermediate complex is spontaneous and the molecular disposition in the reactant complex formed is so favourable that the C–C bond formation occurs readily. On the other hand, with [diamine-B]BF_4, in which the two positively charged NH centres in the methylene carbanion intermediate are separated by increasing the hydrocarbon chain between the two nitrogen atoms, both the transition state and the intermediate of the first step are stabilised and the activation barrier decreases to approximately 2 kcal mol^{-1}. However, co-adsorption of benzaldehyde on the methylene carbanion intermediate complex and its activation to react and form the condensation product is energetically and entropically disfavoured, so that step 2 becomes the rate-determining step. The kinetic study and the agreement between the experimental and calculated activation energies and the isokinetic point confirm the proposed bi-site two-step mechanism, and explain the different behaviour of the two catalysts in terms of the change in the rate-determining step that occurs when the distance between the acidic and basic sites is modified.

Experimental Section

[Diamine-A]BF_4: A 100 mL round-bottomed flask was charged with dipiperidinomethane (10 g, 54.85 mmol) and diethyl ether (30 mL). Then equimolar amounts of tetrafluoroboric acid/diethyl ether were added dropwise into an ice bath. The mixture was stirred at room temperature for 1 h. A solid was formed. It was recovered by filtration and was washed exhaustively with diethyl ether. The solid was dried under vacuum to give the organic salt as a yellow solid (8.1 g, 55 %). ^{1}H NMR (300 MHz, $CDCl_3$): $\delta = 1.5$ (brs), 1.65 (brs), 2.85 (brs), 3.65 ppm (s); ^{13}C NMR (300 MHz, $CDCl_3$): $\delta = 22.5$, 23.9, 51.0, 79.8 ppm; MS (FAB$^+$): m/z: 98 $[M-(C_5H_{11}N)]^+$, 86 $[M-(C_6H_{11}N)]^+$; FTIR: $\tilde{\nu} = 3153$ (s), 2937 (s), 2853 (s), 2800 (s), 1479 (m), 1453 (m), 1311 (w), 1116 (s), 1069 (vs), 1006 (vs), 511cm^{-1} (w); water content (<0.3 %); fluorine composition (%): 27.8 [$C_{11}H_{23}N_2BF_4$ requires 28.0 %].

[Diamine-B]BF_4: A 100 mL round-bottomed flask was charged with 1, 2-di(*N*-piperidine)ethane (5.0 g, 25.47 mmol) and diethyl ether (30 mL). Then equimolar amounts of tetrafluoroboric acid/diethyl ether were added dropwise into an ice bath. The mixture was stirred at room temperature for 1 h. A solid was formed. It was recovered by filtration and was washed exhaustively with diethyl ether. The solid was dried under vacuum to give the organic salt as a yellow solid (4.25 g, 58.7 %). ^{1}H NMR (300 MHz, CD_3CN): $\delta = 1.65$ (brs), 1.75 (brs), 2.85 (brs), 2.9 (s), 5.6 ppm (s); ^{13}C NMR (300 MHz, CD_3CN): $\delta = 22.2$, 23.6, 52.0, 53.3 ppm; MS (FAB$^+$): m/z: 197 $[M-BF_4^-]^+$, 112 $[M-(BF_4^-)-(C_5H_{11}N)]^+$, 98 $[M-(BF_4^-)-(C_6H_{13}N)]^+$; FTIR: $\tilde{\nu} = 3137$ (m), 2932 (s), 2858 (m), 2784 (w), 1458 (m), 1284 (w), 1121 (s), 1063 cm^{-1} (vs).

[*N*-Methyl piperidinium]BF_4: A 50 mL round-bottomed flask was charged with *N*-methyl piperidine (1 g, 50.41 mmol) and diethyl ether (5 mL). Then equimolar amounts of tetrafluoroboric acid/diethyl ether were added dropwise into an ice bath and the mixture was stirred at room temperature for 1 h. Active carbon was added and the reaction mixture was filtered off. Solvent was evaporated under vacuum and the viscous liquid was dried under vacuum to give the protonated compound (3.39 g, 90 %). ^{1}H NMR (300 MHz, $CDCl_3$): $\delta = 1.5$ (s), 1.8 (s), 2.8 (s), 3.05 ppm (m); ^{13}C NMR (300 MHz, $CDCl_3$): $\delta = 55.6$, 44.2, 23.4, 21.0 ppm; MS (FAB$^+$): m/z: 100 $[M-BF_4^-]^+$, 84 $[M-CH_3-BF_4^-]^+$; FTIR: $\tilde{\nu} = 3575$ (m), 3170 (s), 2960 (s), 2863 (s), 2576 (w), 2530, 1839, 1634, 1465 (vs), 1409 (vs), 1276 (m), 1122 (br), 846, 768, 518 (s), 456, 410 cm^{-1}.

Experimental techniques: NMR spectra were recorded using a Bruker Avance 300 spectrometer at 300.13 (^{1}H), 75.47 (^{13}C) and 128 MHz (^{11}B), in deuterated solvents with TMS as an internal standard. FTIR spectra were recorded using a Nicolet 710 FT spectrophotometer in the range of 300–4000 cm^{-1}. Solutions of the respective organic salts in acetonitrile were deposited onto a flat disk of monocrystalline Ge (provided by Sorem-France). After slow solvent evaporation under a nitrogen flow, the spectra were recorded at room temperature. Fast-atom-bombardment (FAB) mass spectra of organic salts were performed with a ditranol matrix using VG-Autospec equipment.

The density of compounds [diamine-A]BF_4, [diamine-B]BF_4 and [*N*-methyl piperidinium]BF_4 was determined using a helium Accupyc 1330 picnometer (cell capacity: 1 cm^3; measurements were taken at 30 °C). Ionic conductivity (σ) measurements were determined using an Orion-160 conductivity meter (conductivity cell model 016010; K (cell constant) = 0.609 cm^{-1}); reference values: Milli-Q-water σ(20 °C): 1 µS cm^{-1}; ethanol σ(20 °C): 0.2 µS cm^{-1}). Decomposition temperatures were obtained by means of thermogravimetric analysis with a SETARAM Setsys Evolution 16/18 thermobalance (10 °C min^{-1}; N_2: 30 mL min^{-1}).

The water content was determined by using the Karl Fischer method and METROHM 702 SM Titrino equipment. The boron content was determined by means of an inductively coupled plasma optical emission spectrometer (ICP-OES) Varian 715-ES in combination with ^{11}B NMR spectroscopy.

General procedure for the Knoevenagel reactions: In a typical experiment, the basic catalysts (0.28 mmol, previously activated for 2 h at 80 °C under vacuum) were added to a solvent-free solution of the methylene compound (4.5 g, 28 mmol) while stirring under an inert atmosphere. After temperature adjustment (80 °C), the aldehydes (3.4 g, 32 mmol) were added and the reaction was periodically monitored by GC.

General procedure for acetalisation of benzaldehyde: In a two-necked 10 mL round-bottomed flask, the catalyst (0.84 mmol) was weighed. Triethyl orthoformate (2.73 mL, 25 mmol) and benzaldehyde (1.05 mL, 10 mmol) were added to the flask with a syringe. The mixture was heated at 130 °C with vigorous stirring for 6 h. During this time several samples were taken, extracted with diethyl ether and analysed by GC.

General procedure for reuse reactions: A normal Knoevenagel reaction was developed with larger amounts of every reactant and catalyst (64 mmol of benzaldehyde, 56 mmol of diethylmalonate and 0.56 mmol of [Amine 1]BF_4). After being left to react for 6 h, products and reactants were extracted with diethyl ether and the viscous yellow catalyst was collected and dissolved in dichloromethane, dried with magnesium sulfate, filtered and evaporated. Finally, the yellow-brown catalyst was dried under vacuum at 40 °C for 2 h.

Dried catalyst was weighed and used for the next reaction (reactants were added in appropriate amount to the catalyst). Five consecutive runs were carried out with the same catalyst using this method.

Computational details: Calculations were carried out by means of the Gaussian 03 program package[36] using the density functional B3PW91 method[37] and the standard 6-31G(d,p) basis set.[38] The geometries of all species considered were fully optimised and the nature of every stationary point was characterised by means of frequency calculations and analysis of the vibrational modes. Additional geometry optimisations starting from the transition states were performed to establish which reactants and products were linked by a specific transition state. Zero-point vibrational energy (ZPE) corrections to the total energies were obtained from frequency calculations.

Acknowledgements

The authors thank CICYT (MAT 2006-14274-C02-01) for financial support.

---

[1] a) T. Welton, *Chem. Rev.* **1999**, *99*, 2071–2083; b) M. J. Earle, K. R. Seddon, *Pure Appl. Chem.* **2000**, *72*, 1391–1398; c) P. Wasserscheid,

W. Keim, *Angew. Chem.* **2000**, *112*, 3926–3945; *Angew. Chem. Int. Ed.* **2000**, *39*, 3772–3789; d) J. Dupont, R. Souza, P. Suarez, *Chem. Rev.* **2002**, *102*, 3667–3692.
[2] a) D. Zhao, M. Wu, Y. Kou, E. Min, *Catal. Today* **2002**, *74*, 157–189; b) Z. C. Zhang, *Adv. Catal.* **2006**, *49*, 153–273.
[3] a) K. Qiao, Y. Deng, *J. Mol. Catal. A: Chem.* **2001**, *171*, 81–84; b) G. Wang, W. Qiao, L. Cheng, *Appl. Catal. A* **2004**, *262*, 69–73.
[4] Y. Deng, F. Dhi, J. Beng, K. Quiao, *J. Mol. Catal. A: Chem.* **2001**, *165*, 33–36.
[5] M. H. Valkenberg, C. de Castro, W. F. Holderich, *Appl. Catal. A* **2001**, *215*, 185–190.
[6] A. Kumar, S. S. Pawar, *J. Mol. Catal. A: Chem.* **2004**, *208*, 33–37.
[7] C. Lee, *Tetrahedron Lett.* **1999**, *40*, 2461–2464.
[8] A. C. Cole, J. L. Jensen, I. Ntai, K. L. T. Tran, K. J. Weave, D. C. Forbes, J. H. Davis, *J. Am. Chem. Soc.* **2002**, *124*, 5962–5963.
[9] Y. Gu, F. Shi, Y. Deng, *Catal. Commun.* **2004**, *5*, 597–601.
[10] F. Gu, Y. Shi, J. Deng, *J. Mol. Catal. A: Chem.* **2004**, *212*, 71–75.
[11] K. Qiao, C. Yokoyama, *Chem. Lett.* **2004**, *33*, 472–473.
[12] a) M. Yoshizawa, W. Xu, C. A. Angell, *J. Am. Chem. Soc.* **2003**, *125*, 15411–15419; b) H. Ohno, M. Yoshizawa, W. Ogihara, *Electrochim. Acta* **2004**, *50*, 255–261.
[13] Z. Du, Z. Li, S. Guo, J. Zhang, L. Zhu, Y. Deng, *J. Phys. Chem. B* **2005**, *109*, 19542–19546.
[14] Z. Duan, Y. Gu, J. Zhang, L. Zhu, Y. Deng, *J. Mol. Catal. A: Chem.* **2006**, *250*, 163–168.
[15] H. P. Zhu, F. Yang, J. Tang, M. Y. He, *Green Chem.* **2003**, *5*, 38–39.
[16] H. H. Wu, F. Yang, P. Cui, J. Tang, M. Y. He, *Tetrahedron Lett.* **2004**, *45*, 4963–4965.
[17] G. Zhao, T. Jiang, H. Gao, B. Han, J. Huang, D. Sun, *Green Chem.* **2004**, *6*, 75–77.
[18] T. L. Greaves, C. J. Drummond, *Chem. Rev.* **2008**, *108*, 206–237.
[19] a) A. R. Gholap, K. Venkatesan, T. Daniel, R. J. Lahoti, K. V. Srinivasan, *Green Chem.* **2003**, *5*, 693–696; b) T. Welton, *Coord. Chem. Rev.* **2004**, *248*, 2459–2477.
[20] a) M. J. Earle, P. B. MacCormac, K. R. Seddon, *Green Chem.* **1999**, *1*, 23–25; b) A. Zhu, T. Jiang, B. Han, J. Huang, J. Zhang, X. Ma, *New J. Chem.* **2006**, *30*, 736–740.
[21] N. Bicak, *J. Mol. Liq.* **2005**, *116*, 15–18.
[22] a) B. C. Ranu, R. Jana, *Eur. J. Org. Chem.* **2006**, 3767–3770; b) J. M. Xu, C. Qian, B. K. Liu, Q. Wu, X. F. Lin, *Tetrahedron* **2007**, *63*, 986–990; c) L. Yang, L. W. Xu, W. Zhou, L. Li, C. G. Xia, *Tetrahedron Lett.* **2006**, *47*, 7723–7726.
[23] D. R. MacFarlane, S. A. Forsyth, J. Golding, G. B. Deacon, *Green Chem.* **2002**, *4*, 444–448.
[24] M. Yoshizawa-Fujita, K. Johansson, P. Newman, D. R. MacFarlane, *Tetrahedron Lett.* **2006**, *47*, 2755–2758.
[25] M. J. Earle, K. R. Seddon, S. Forsyth, U. Frohlich, N. Gunaratne, S. Katdare, WO 2006/072775, **2006**.
[26] A. Noda, M. Susan, K. Kudo, S. Mitsushima, K. Hayamizu, M. Watanabe, *J. Phys. Chem. B* **2003**, *107*, 4024–4033.
[27] a) H. A. Staab, T. Saupe, *Angew. Chem.* **1988**, *100*, 895–909; *Angew. Chem. Int. Ed. Engl.* **1988**, *27*, 865–909; b) A. L. Llamas-Saiz, C. Foces-Foces, J. Elguero, *J. Mol. Struct.* **1994**, *328*, 297–323.
[28] I. Rodriguez, G. Sastre, A. Corma, S. Iborra, *J. Catal.* **1999**, *183*, 14–23.
[29] M. J. Climent, A. Corma, I. Dominguez, S. Iborra, M. J. Sabater, *J. Catal.* **2007**, *246*, 136–146.
[30] A. Corma, S. Iborra, I. Rodriguez, F. Sanchez, *J. Catal.* **2002**, *211*, 208–215.
[31] G. Jones in *Organic Reactions, Vol. 15* (Ed.: A. C. Cope), Wiley, New York, **1967**, p. 204.
[32] O. Attanasi, P. Filippone, A. Mei, *Synth. Commun.* **1983**, *13*, 1203–1208.
[33] R. P. Shanthan Rao, R. V. Venkataratnam, *Tetrahedron Lett.* **1991**, *32*, 5821–5822.
[34] W. Bao, Y. Zhang, J. Wang, *Synth. Commun.* **1996**, *26*, 3025–3028.
[35] a) M. J. Climent, A. Corma, V. Fornes, R. Guil-Lopez, S. Iborra, *Adv. Synth. Catal.* **2002**, *344*, 1090–1096; b) M. J. Climent, A. Corma, S. Iborra, A. Velty, *J. Mol. Catal. A: Chem.* **2002**, *182–183*, 327–342.
[36] Gaussian 03, Revision B.04, M. J. Frisch, G. W. Trucks, H. B. Schlegel, G. E. Scuseria, M. A. Robb, J. R. Cheeseman, J. A. Montgomery, Jr., T. Vreven, K. N. Kudin, J. C. Burant, J. M. Millam, S. S. Iyengar, J. Tomasi, V. Barone, B. Mennucci, M. Cossi, G. Scalmani, N. Rega, G. A. Petersson, H. Nakatsuji, M. Hada, M. Ehara, K. Toyota, R. Fukuda, J. Hasegawa, M. Ishida, T. Nakajima, Y. Honda, O. Kitao, H. Nakai, M. Klene, X. Li, J. E. Knox, H. P. Hratchian, J. B. Cross, V. Bakken, C. Adamo, J. Jaramillo, R. Gomperts, R. E. Stratmann, O. Yazyev, A. J. Austin, R. Cammi, C. Pomelli, J. W. Ochterski, P. Y. Ayala, K. Morokuma, G. A. Voth, P. Salvador, J. J. Dannenberg, V. G. Zakrzewski, S. Dapprich, A. D. Daniels, M. C. Strain, O. Farkas, D. K. Malick, A. D. Rabuck, K. Raghavachari, J. B. Foresman, J. V. Ortiz, Q. Cui, A. G. Baboul, S. Clifford, J. Cioslowski, B. B. Stefanov, G. Liu, A. Liashenko, P. Piskorz, I. Komaromi, R. L. Martin, D. J. Fox, T. Keith, M. A. Al-Laham, C. Y. Peng, A. Nanayakkara, M. Challacombe, P. M. W. Gill, B. Johnson, W. Chen, M. W. Wong, C. Gonzalez, J. A. Pople, Gaussian, Inc., Wallingford CT, **2004**.
[37] a) A. D. Becke, *J. Chem. Phys.* **1993**, *98*, 5648–5652; b) J. P. Perdew, Y. Wang, *Phys. Rev. B* **1992**, *45*, 13244–13249.
[38] P. C. Hariharan, J. A. Pople, *Theor. Chim. Acta* **1973**, *28*, 213–222.

Received: June 4, 2009